doi: 10.1038/nature07931

METHODS

Nd-LSCO. Single crystals of $La_{1.6-x}Nd_{0.4}Sr_xCuO_4$ (Nd-LSCO) were grown at the University of Texas using a travelling float zone technique. *ab*-plane single crystals were cut from boules with nominal Sr concentrations $x = 0.20$ and $x = 0.25$. The actual doping p of each crystal was estimated from its T_c and ρ(250 K) values compared with published data, giving $p = 0.20 \pm 0.005$ and 0.24 ± 0.005, respectively.

Eu-LSCO. Single crystals of $La_{1.8-x}Eu_{0.2}Sr_xCuO_4$ (Eu-LSCO) were grown at the University of Tokyo using a travelling float zone technique, with Sr concentrations $x = 0.125$ and $x = 0.16$. The doping p is taken to equal the Sr content x, to within ± 0.005. The physical dimensions of the *ab*-plane samples cut out of the single-crystal boules were measured using an optical microscope and are shown in Table 1. The length L is measured between the contacts used to measure the temperature difference or voltage drop along the current direction (x-axis).

Table 1

Sample	**Length, *L* [mm]**	**Width, *w* [mm]**	**Thickness, *t* [mm]**
Eu-LSCO x=0.125	0.94 ± 0.10	0.28 ± 0.02	0.19 ± 0.02
Eu-LSCO x=0.16	0.45 ± 0.10	0.43 ± 0.02	0.23 ± 0.02
Nd-LSCO x=0.20	1.51 ± 0.05	0.50 ± 0.02	0.64 ± 0.02
Nd-LSCO x=0.25	2.50 ± 0.05	0.51 ± 0.02	0.51 ± 0.02

Superconducting transition temperature T_c. The superconducting transition temperature T_c of our Nd / Eu-LSCO samples was determined via resistivity measurements. In Table 2, we give T_c values for two different criteria: 1) the temperature where the resistivity goes to zero; 2) the midpoint of the transition.

Table 2

Sample	T_c [K] (ρ = 0)	T_c [K] (midpoint ρ)
Eu-LSCO x=0.125	5 ± 2	8 ± 4
Eu-LSCO x=0.16	16 ± 3	24 ± 5
Nd-LSCO x=0.20	20 ± 1	23 ± 3
Nd-LSCO x=0.25	17 ± 1	20 ± 3

Contacts. Electrical contacts on the Eu / Nd-LSCO samples were made to the crystal surface using Epo-Tek H20E silver epoxy. This epoxy was cured for 5 min at 180 C then annealed at 500 C in flowing oxygen for 1 hr so that the silver diffused into the surface. This resulted in contact resistances of less than 0.1 Ω at room temperature. The longitudinal contacts were wrapped around all four sides of the sample. The current contacts covered the end faces. Nernst / Hall contacts were placed opposite each other in the middle of the samples, extending along the length of the *c*-axis, on the sides. The uncertainty in the quoted length L of the sample (between longitudinal contacts) reflects the width of the voltage / temperature contacts along the *x*-axis.

Measurement of the Nernst coefficient. The Nernst signal was measured by applying a steady heat current through the sample (along the *x*-axis). The longitudinal thermal gradient was measured using two uncalibrated Cernox chip thermometers (Lakeshore), referenced to a further calibrated Cernox. The transverse electric field was measured using nanovolt preamplifiers and a nanovoltmeter. The temperature of the experiment was stabilized at each point to within ±10 mK. The temperature and voltage were measured with and without applied thermal gradient (ΔT) for calibration. The magnetic field B, applied along the *c*-axis ($B \parallel z$), was then swept, with the heat on, from – 10 to + 10 T at 0.35 T / min, continuously taking data. The thermal gradient was monitored continuously and remained constant during the course of a sweep. The Nernst coefficient (N) was extracted from the part of the measured voltage antisymmetric with respect to magnetic field:

$$N = E_y / (\partial T / \partial x) = [\Delta V_y(B) / \Delta T_x - \Delta V_y(-B) / \Delta T_x] (L / 2 w) ,$$

where ΔV is the difference in the voltage measured with and without thermal gradient. L is the length (between contacts along the x-axis) and w the width (along the y-axis) of the sample. This anti-symmetrization procedure removes any thermoelectric contribution from the sample or from the rest of the measurement circuit.

Extraction of T_ν. We define T_ν as the point where ν / T deviates from linearity at high temperature; see Figures S2 and S5. This criterion is based on the fact that ν / T is linear in T at all T in Nd-LSCO at $p = 0.24 > p^*$, our reference sample where there is neither superconducting contribution to the Nernst signal nor any Fermi-surface reconstruction. This qualitative definition allows us to identify T_ν unambiguously to within +/- 10 K.

Measurements of resistivity and Hall coefficient. The resistivity $\rho(T) \equiv R_{xx}\, w\, t / L$ and Hall coefficient $R_H(T) \equiv R_{xy}\, t / B$ of each sample were measured using the standard six-terminal AC technique. A resistance bridge or a lock-in amplifier was used to measure the resistance. Field reversal was used to obtain the symmetric and anti-symmetric parts of the voltages, accounting for any misalignment of the contacts. Therefore, the longitudinal (R_{xx}) and transverse (R_{xy}) resistances were obtained as follows:

$$R_{xx} = (R(B) + R(-B)) / 2 \quad \text{and} \quad R_{xy} = (R(B) - R(-B)) / 2.$$

Measurements of hard X-ray diffraction. Hard X-ray diffraction measurements were performed with the BL19LXU beamline at RIKEN SPring-8. The photon energy was tuned to 24 keV. Q-scan profiles along the *h* direction revealed a broad superstructure reflection at (4-2ε, 0, 0.5) with 2ε = 0.238(5) at low temperatures, indicative of stripe charge ordering. The peak was modelled with a Gaussian, assuming a linear background.

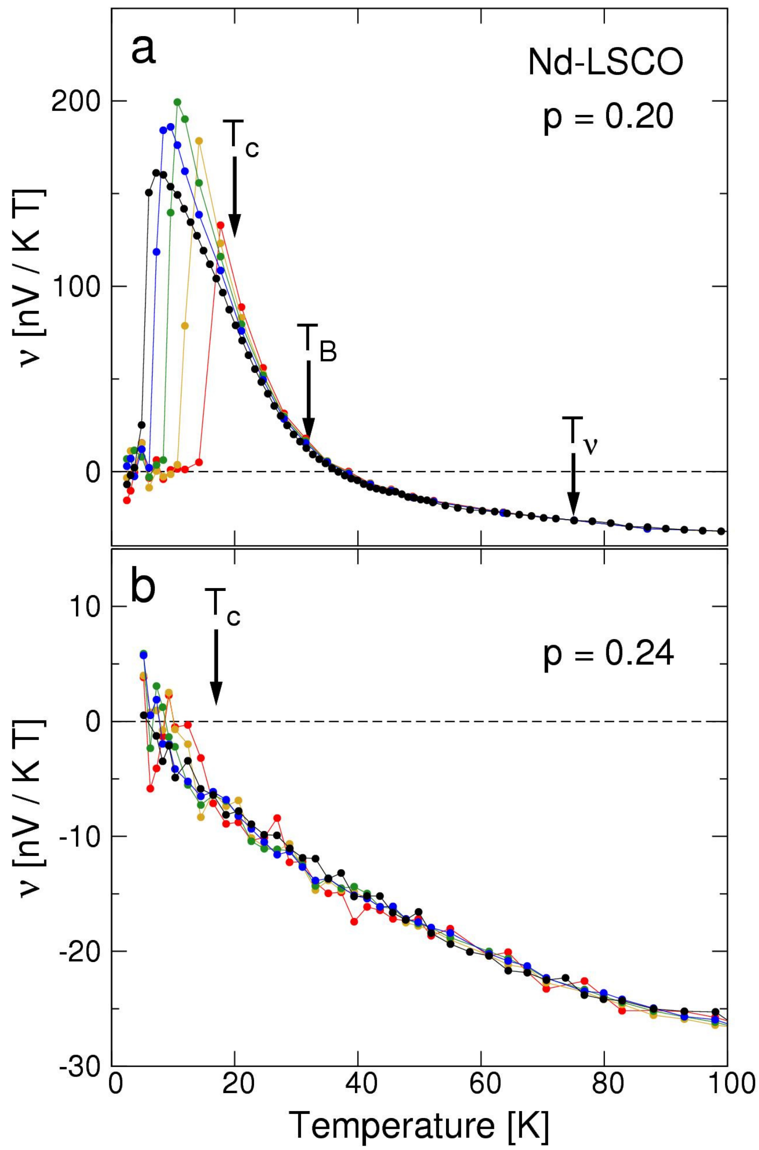

Figure S1 | Effect of a magnetic field on the Nernst coefficient of Nd-LSCO.

Nernst coefficient ν as a function of temperature for Nd-LSCO at $p = 0.20$ (upper panel) and $p = 0.24$ (lower panel), for different magnetic field strengths: $B = 2$ T (red), 4 T (yellow), 6 T (green), 8 T (blue), 10 T (black). T_c is the zero-field superconducting transition (where $\rho = 0$). For $p = 0.20$, the onset of field dependence is labelled T_B. At higher temperature, ν / T becomes linear in temperature above T_ν (see Fig. S2). By contrast, for $p = 0.24$, the field dependence is within the noise of the measurement down to T_c and both T_B and T_ν are indistinguishable from zero.

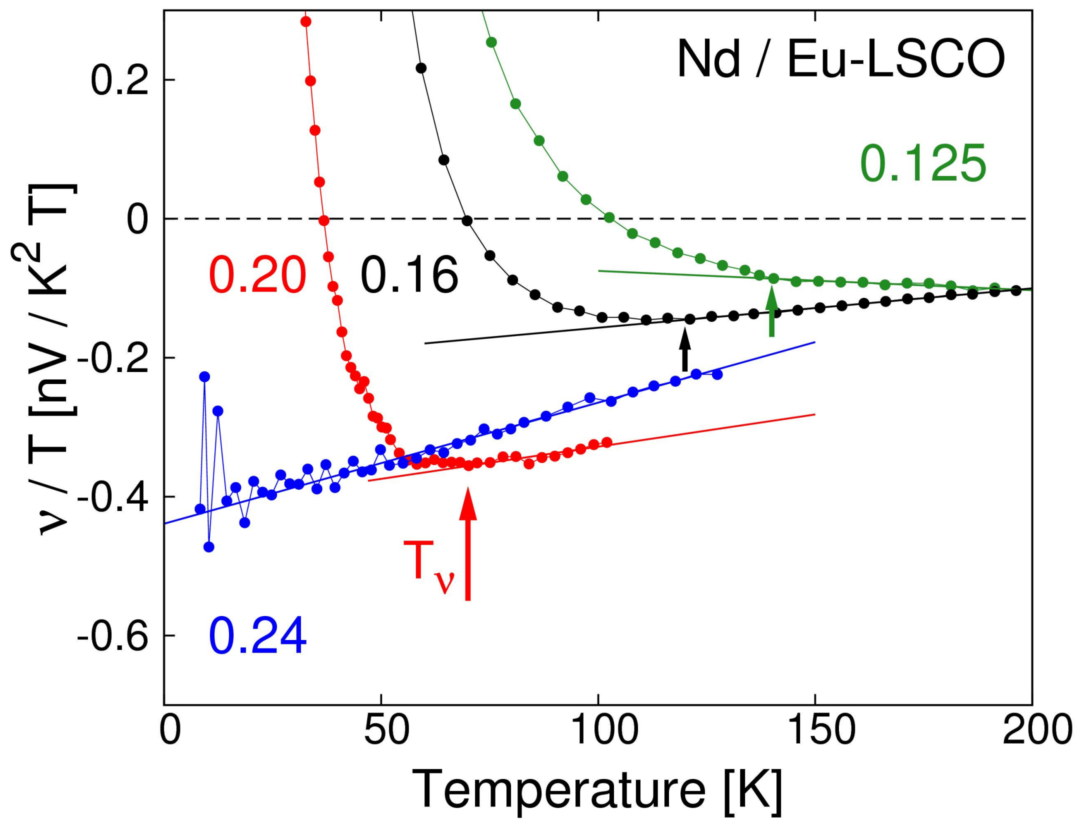

Figure S2 | Onset of the positive upturn in the Nernst coefficient.

Nernst coefficient ν divided by temperature T for Eu-LSCO at p = 0.125 (green) and p = 0.16 (black), and for Nd-LSCO at p = 0.20 (red) and p = 0.24 (blue). All curves are taken in 10 T. The onset temperature T_ν (arrows) is defined as the deviation of ν / T from a linear fit at high temperature. This yields T_ν = 140 ± 10, 120 ± 10, 70 ± 10 and 0 K, respectively.

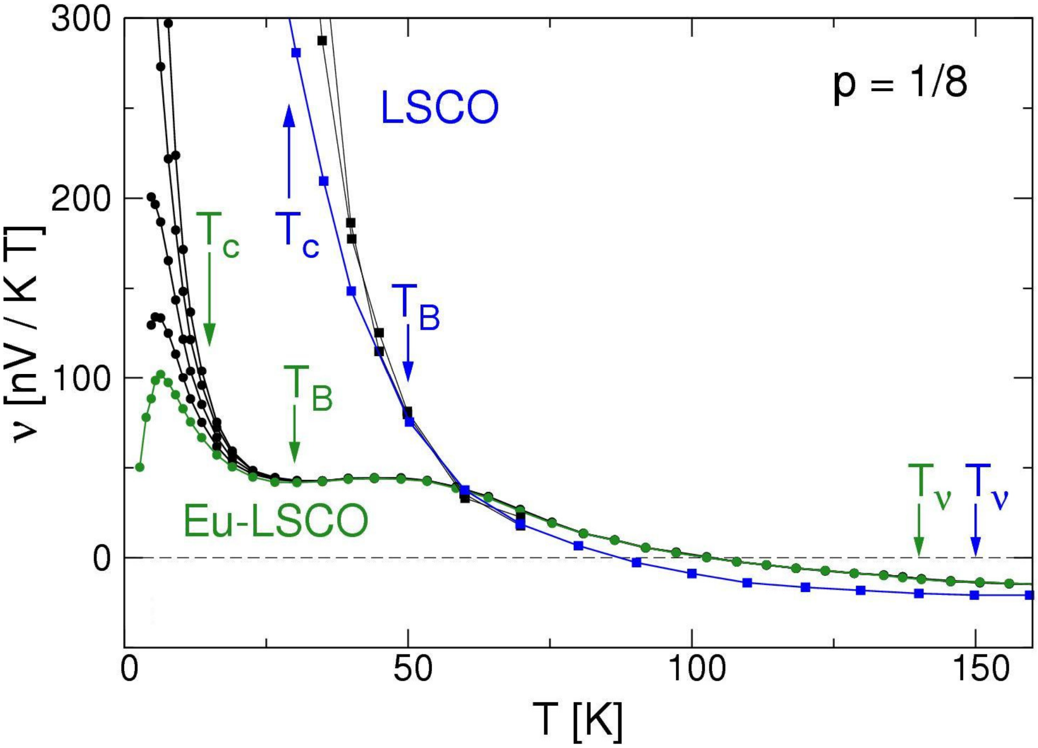

Figure S3 | Comparison of Nernst coefficient in Eu-LSCO vs LSCO.

Temperature dependence of the Nernst coefficient $\nu(T)$ for different magnetic fields in Eu-LSCO at $p = 0.125$ [circles] and LSCO at $p = 0.12$ [squares; from ref. 1]. Field strengths are 2, 4, 6, 8 and 10 T for Eu-LSCO (top to bottom), and 1, 6 and 14 T for LSCO (top to bottom). T_ν marks the onset of the positive rise at high temperature, as defined in Supplementary Figs. S2 and S5. T_B marks the onset of a field dependence in $\nu(T)$, the expected signature of superconducting fluctuations. T_c marks the onset of the superconducting transition in the zero-field resistivity. Note how $\nu(T)$ in Eu-LSCO exhibits two separate peaks, at 7 K and 45 K, which we attribute respectively to superconducting fluctuations (characterized by a strong field dependence) and quasiparticles (no field dependence), with respective onsets at T_B and T_ν. In LSCO at the same doping, the rise in $\nu(T)$ at high temperature is very similar, but the low-temperature field-dependent rise has moved up in temperature, with T_B tracking T_c.

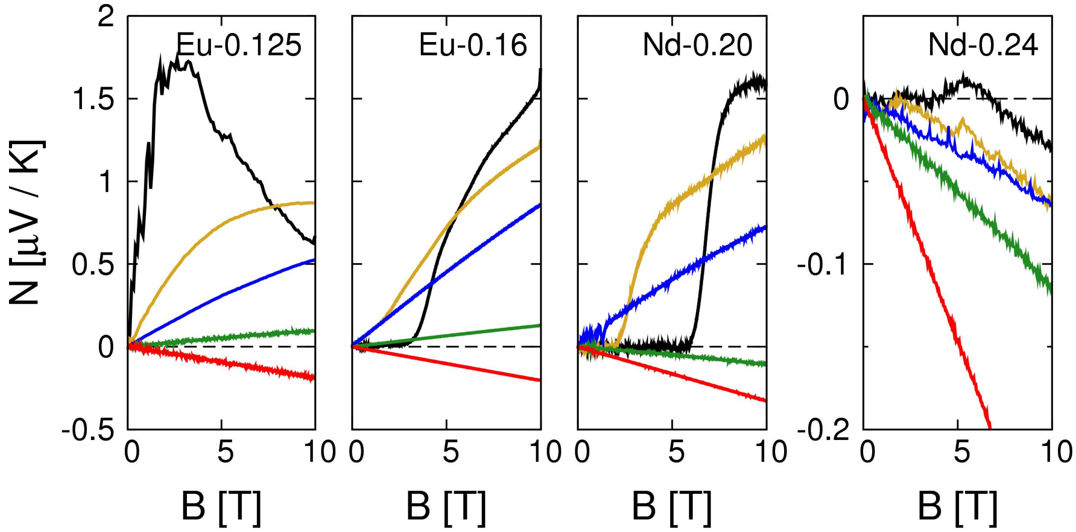

Figure S4 | Magnetic field dependence of the Nernst signal.

Field dependence of the Nernst signal in the four samples of Eu / Nd-LSCO measured in this study, at several temperatures: above T_v [red]; between T_v and T_B (the onset of non linearity in N vs B) [green]; between T_B and the midpoint of the zero-field superconducting transition, T_c [blue]; below T_c [yellow and black]. The temperature of each curve is, respectively : 184, 83.6, 17.6, 9.7, 3.4 K (p = 0.125); 196, 59.2, 32.0, 18.6, 7.2 K (p = 0.16); 106, 45.4, 21.1, 14.2, 8.4 K (p = 0.20); 132, 28.9, 16.5, 12.4, 8.3 K (p = 0.24).

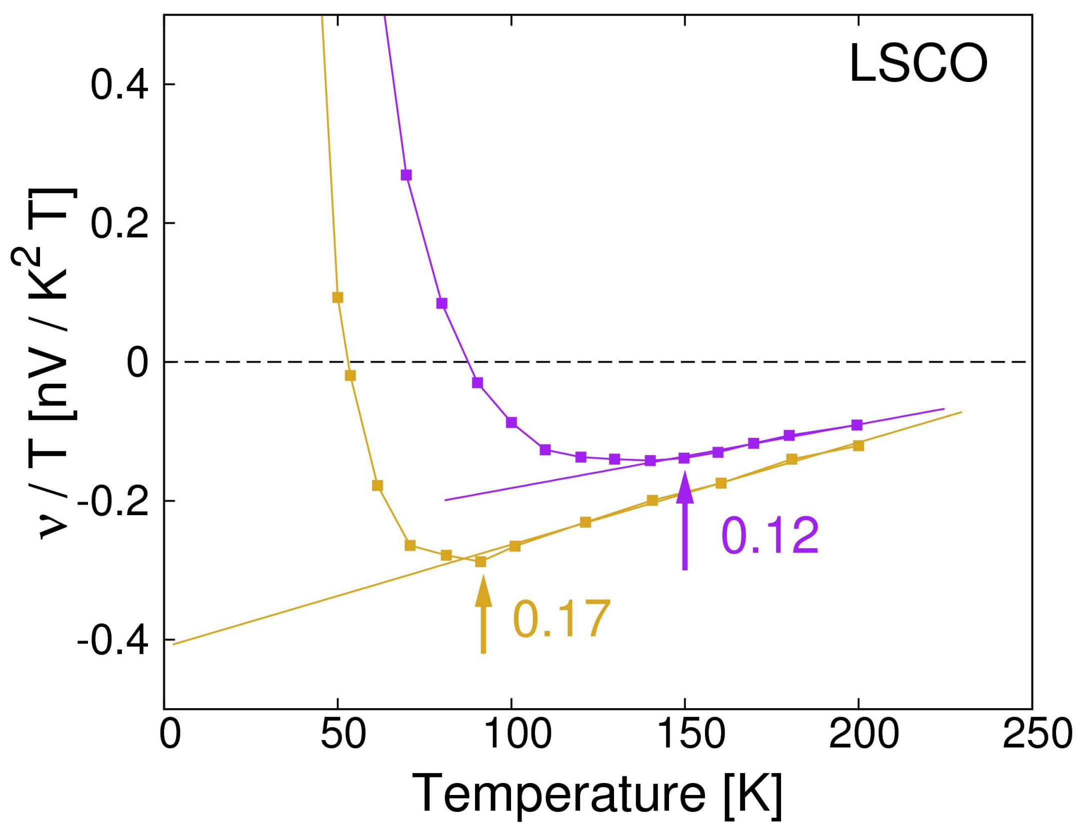

Figure S5 | Onset of the positive upturn in the Nernst coefficient in LSCO.

Nernst coefficient *ν* divided by temperature *T* for LSCO at *p* = 0.12 (purple) and *p* = 0.17 (yellow) (from refs. 1, 2, and 3). Both curves show the zero field limit; there is no evidence of field dependence above 60 K. The onset temperature T_{ν} is defined as the deviation of *ν* / *T* from a linear fit at high temperature, giving T_{ν} =150 ± 10 and 90 ± 10 K, respectively.

[1] Wang, Y., Li, P. & Ong, N.P. *Phys. Rev. B* **73,** 024510 (2006).

[2] Ong, N.P. *et al*., *Ann. Phys. (Leipzig)* **13**, 9-14 (2004).

[3] Wang, Y. *et al*., *Phys. Rev. Lett.* **88,** 257003 (2002).